31st Congress of the International Council of the Aeronautical Sciences

Belo Horizonte, Brazil; September 09-14, 2018

NONLINEAR AEROELASTIC REDUCED ORDER MODELS USING MODAL COORDINATES

Renato R. Medeiros* , **Carlos E. S. Cesnik*** , **and Etienne B. Coetzee****
***University of Michigan** , ****Airbus Operations**

Keywords: *aeroelasticity, reduced order models, modal coordinates*

Abstract

This paper presents an aeroelastic reduced order tool to analyze very flexible structures. It is based on different model reduction techniques for the structural and the aerodynamic problems. The structural reduced order model is the Implicit Condensation and Expansion technique that was recently extended to incorporate large displacements, while the aerodynamic model is based on the method of segments. Results are presented comparing the aeroelastic response for a high-aspect-ratio wing considering both the reduced order approach and higher-fidelity solutions.

1 Introduction

In the recent decades, reduced order models (ROMs) have shown a potential to greatly reduce computational costs. Both structural and aerodynamic ROMs have been developed, but these models are not always applicable to the large displacements experienced by high-aspect-ratio wings. The main tools used for development of very flexible aircraft are currently based on beam solutions and strip theory or lifting-line aerodynamics, like UM/NAST [1] and ASWING [2]. These codes incorporate the nonlinear aspects of large displacements and are fast enough to allow time-domain evaluations under multiple flight conditions. However, the pre-processing step of extracting equivalent beams and the aerodynamic simplifications of these methods add to an overall reduction of accuracy. The idea of nonlinear ROMs based on modal coordinates is to bypass the generation of equivalent beams, creating a model directly derived from the complete FEM with a higher accuracy and lower order.

Recent developments have extended the capabilities of structural nonlinear ROMs to large displacements. Previous ROMs had included nonlinear stiffness and displacement terms for shells undergoing vibrations with amplitude on the order of the plate thickness. Example of such can be found in the work of McEwan *et al.* [3] that proposed the Implicit Condensation method. This approach uses the modal coordinates as degrees of freedom and the identification of parameters is performed by exciting the structure statically with loads in the shape of the first few linear modes to get the nonlinear stiffness terms. Additional cubic terms are necessary to model nonlinear displacements, as demonstrated by Mignolet *et al.* [4] using a Galerkin method. For a more complete representation of displacements, the idea of dual modes was introduced by Hollkamp and Gordon [5], with the Implicit Condensation and Expansion (ICE) technique. The ICE methodology refined the displacement recovery for shell-like structures, but the large wing deflections experienced by models like the NASA Helios [6] and the University of Michigan's X-HALE [7] in dynamic conditions could not be captured without higher-order stiffness terms. The work of Ritter *et al.* [8] introduced the Enhanced Modal Approach (EnMA), based on Taylor expansion for nonlinear displacements and potential energy. This framework achieved high accuracy for steady simulations with high displacements. Finally, the authors [9] expanded

the ICE method to account for the nonlinear displacements and inertia terms while keeping the higher-order stiffness and displacement terms of the EnMA.

Aerodynamic ROMs have made CFD computations more accessible by using tools such as Proper Orthogonal Decomposition (POD) and identification techniques. The review paper of Taira *et al.* [10] summarizes the main methods currently available for aerodynamic ROMs, which are broadly classified as projection-based methods, working with the residual equations, and output-based approaches, which are based on input/output system identification. For dynamic aeroelastic simulations, the calculation of aeroelastic forces using output-based methods can be achieved with various different techniques, among them recurrent neural networks [11] and POD [12]. However, the focus of this work is the method of segments (MoS), which uses linear convolution and a correction factor from a limited set of nonlinear simulations to predict the loads along different sections of the wing. This is a relatively simple method that can achieve good accuracy for high-aspect-ratio configurations. Its performance was demonstrated in the work of Skujins and Cesnik [13], which successfully used it with the AGARD 445.6 wing across multiple Mach regimes.

In a previous paper from the authors [14], a structural ROM developed to model large displacements was directly integrated with the CFD code CFL3D [15], verifying the capability of nonlinear structural modeling in a high-fidelity framework. This work replaces the CFD code with the method of segments, reducing the cost of the analysis. The objective is to evaluate the accuracy of the MoS in steady and unsteady aeroelastic simulations, comparing the results against reference solutions obtained with the CFL3D/ICE framework developed previously.

The following section summarizes the formulation for both the enhanced ICE nonlinear structural reduced order model and the aerodynamic MoS. A 16-m wing structure used for all comparisons is presented and verification cases for the structural ROM are discussed. Finally, in the results section, aeroelastic static and dynamic simulations for the MoS/ICE framework are compared against reference data obtained with the CFL3D/ICE method.

2 Formulation

The formulation of each of the two components that make the nonlinear aeroelastic framework are summarized here.

2.1 Implicit Condensation and Expansion Structural ROM

The ICE is based on modal coordinates related to the first few linear modes, which are the degrees of freedom for the nonlinear ROM. However, the displacement is represented using both the linear mass-normalized elastic modes Φ of the undeformed structure and an additional displacement basis called dual modes, Ψ. The dual modes are not elastic modes of the structure. They are only mathematical bases that augment the space of possible displacements to include nonlinear features that are not represented by linear modes, like beam shortening at high deflections. The array of displacements u is represented as a combination of linear modes and dual modes with amplitudes q and r, respectively, such as

$$u = \Phi q + \Psi r(r) \tag{1}$$

where the amplitude of dual modes is a function of the amplitude of linear modes. This is one of the key hypothesis of the ICE method: that the displacement is completely determined by the amplitudes of the linear modes, which are the only degrees of freedom of the system. Under this hypothesis, the equations of motion are derived from the Euler-Lagrange equations, i.e.,

$$\frac{d}{dt}\left(\frac{\partial T}{\partial \dot{q}_i}\right) - \frac{\partial T}{\partial q_i} + \frac{\partial U}{\partial q_i} = F^T \frac{\partial u}{\partial q_i} \quad \text{for} \quad i = 1, \ldots, n \tag{2}$$

where T represents the kinetic energy and U is the elastic potential energy. F is the array of external loads and u is the array of displacements,

which are related to the n degrees of freedom q_i through Eq. 1.

It is important to notice that the velocity is related to both linear and dual modes. At large displacements, the contribution from the dual modes to the kinetic energy is essential to keep the accuracy of ICE predictions. The kinetic energy is ultimately written as

$$T = \frac{1}{2}\dot{q}^T \underbrace{\left(I_n + 2M_X\frac{\partial r}{\partial q} + \frac{\partial r}{\partial q}^T M_\Psi \frac{\partial r}{\partial q}\right)}_{M'} \dot{q} \quad (3)$$

where I_n is an identity matrix of size $n \times n$ and the terms M_X and M_Ψ are defined as

$$\Phi^T M \Psi = M_X \quad (4)$$

$$\Psi^T M \Psi = M_\Psi \quad (5)$$

where M is the mass matrix of the structure. Eq. 3 shows that the contribution of dual modes to the motion may be accounted for in a modified mass matrix M'.

For large displacements, the potential energy assumes a nonlinear form, i.e.,

$$\frac{\partial U}{\partial q} = \Lambda q + \frac{\partial U_{nl}}{\partial q} \quad (6)$$

where Λ is the diagonal matrix of eigenvalues of the system and $\frac{\partial U_{nl}}{\partial q}$ is the array of nonlinear elastic forces. Replacing the kinetic energy in the Euler-Lagrange equations (Eq. 2), it is possible to express the equations of motion as function of the degrees of freedom q and the first and second derivatives of the function $r(q)$ that relates the amplitudes of dual modes and linear modes, as well as the nonlinear elastic forces $\frac{\partial U_{nl}}{\partial q}$, i.e.,

$$\begin{aligned}
&\left(I_n + M_X\frac{\partial r}{\partial q} + \frac{\partial r}{\partial q}^T M_X^T + \frac{\partial r}{\partial q}^T M_\Psi \frac{\partial r}{\partial q}\right)\ddot{q} + \\
&\left[M_X\frac{d}{dt}\frac{\partial r}{\partial q} + \frac{d}{dt}\frac{\partial r}{\partial q}^T M_X^T + \frac{d}{dt}\frac{\partial r}{\partial q}^T M_\Psi \frac{\partial r}{\partial q} + \right. \\
&\frac{\partial r}{\partial q}^T M_\Psi \frac{d}{dt}\frac{\partial r}{\partial q} - \\
&\left.\left[\dot{q}^T\left(M_X + \frac{\partial r}{\partial q}^T M_\Psi\right)\left(\frac{\partial^2 r}{\partial q^2}\right)_{s\times n^2}\right]^T_{n\times n}\right]\dot{q} \\
&= \left(\Phi + \Psi\frac{\partial r}{\partial q}\right)^T F - \Lambda q - \frac{\partial U_{nl}}{\partial q}
\end{aligned} \quad (7)$$

where the subscript indices $s \times n^2$ and $n \times n$ indicate reshaping of the corresponding matrices. $\left(\frac{\partial^2 r}{\partial q^2}\right)_{s\times n^2}$ represents the second derivative of the dual mode amplitudes, with s rows and n^2 columns, where s is the number of dual modes and n is the number of linear modes. Specifically,

$$\left(\frac{\partial^2 r}{\partial q^2}\right)_{s\times n^2} = \left[\frac{\partial^2 r}{\partial q_1 \partial q} \quad \frac{\partial^2 r}{\partial q_2 \partial q} \cdots \frac{\partial^2 r}{\partial q_n \partial q}\right] \quad (8)$$

where each $\frac{\partial r}{\partial q}$ is a $s \times n$ matrix with each column representing the derivate of r with respect to a different modal amplitude. Equation 7 is the set of equations of motion.

From the formulation above, two functions need prior identifications using nonlinear static solutions: the nonlinear elastic forces $\frac{\partial U_{nl}}{\partial q}$ and the amplitudes of the dual modes $r(q)$. For this identification process, combinations of loads in the shape of linear modes is applied to the structure, with different amplitudes, resulting in displacements from which the linear contribution of linear modes is subtracted, leaving a residue from which the dual modes are calculated using singular value decomposition, like in a POD process. Using nonlinear solutions as snapshots for both the nonlinear displacements and nonlinear elastic forces, a fitting relates these terms to the amplitudes of the linear modes. Any suitable fitting may be employed, but in this case a set of neural networks was used for all fittings. More details

about this process are described in Medeiros *et al.* [14, 16].

2.2 Method of Segments

For the aerodynamic solution, the MoS was selected. This procedure uses high-fidelity solutions for the calculation of steady loads related to different segments of the wing at a given Mach and angle of attack. Following this approach, the effects of induced local velocities are included, considering the reference deformation state chosen for the CFD computations.

The unsteady loads are included using linear convolution of the step modal and angle of attack responses. CFD codes are able to calculate solutions for step motions if the amplitudes are sufficiently small. Then, using the high-fidelity step responses, it is possible to calculate the unsteady linear modal forces for any deformation. However, in order to correct for the nonlinearities related to high displacements, the unsteady linear loads are adjusted using a correction factor which is the ratio of a nonlinear steady response and a linear steady one, such as

$$f_c = \frac{y_{NL,steady}}{y_{Lin,steady}} \tag{9}$$

where y represents any scalar output of the aerodynamic solution, e.g., a modal force or an aerodynamic coefficient.

The implementation of the MoS follows a few steps in the off-line computation:

- Choose a reference configuration (deformation state) for the calculation of the nonlinear steady solutions;
- Obtain steady solutions at different angles of attack and velocities using a CFD code;
- Sub-divide the wing in different span-wise segments and calculate loads for each segments using the steady solutions obtained;
- Fit the loads (lift, drag and moments) for each segment of the wing as a function of angle of attack and velocity or Mach number;
- Obtain unsteady solutions for step inputs of angle of attack and modal deformation, around the reference configuration. Calculate the required outputs for the aeroelastic computations at this stage, such as modal forces and global aerodynamic coefficients.

From the off-line computations, the steady loads acting on each segment are known for any angle of attack and velocity. One of the main approximation hypothesis of the MoS is that the loads at any considered deformation state will be a function of the local geometric angle of attack and flow velocity only. This assumption neglects the fact that deformations of the wing will induce different velocities on a given segment. However, as will be shown, this approximation can achieve good results for high-aspect-ratio wings.

For an aeroelastic computation, the unsteady aerodynamic loads from the MoS are considered using a convolved linear unsteady solution with a correction factor adjustment. That is a second assumption of the MoS: the amplitude of unsteady nonlinear loads can be corrected using the steady correction factor dependent on the current instantaneous deformation state.

The on-line stage of the method of segments can be described using the following procedure at each time step of the solution:

- From the history of modal deformations and angles of attack, evaluate the outputs of interest via convolution, using the database of linear step responses;
- Use the current deformation state to calculate the local geometric angle of attack of each segment, and use that information to fit the nonlinear steady loads related to that segment;
- Calculate the outputs of interest such as modal forces from the loads of all the segments along the wing. These results will be the nonlinear steady solution used for the computation of the correction factor;

- Compute the linear steady solution using the current deformation state and angle of attack, and the final values of the step responses in the database;
- Get the correction factor from the ratio of the nonlinear steady and linear steady responses;
- Multiply the convolved unsteady linear response by the respective correction factor in order to obtain the approximated unsteady nonlinear loads to be transferred to the structure.

More details about the method of segments can be found in the work of Skujins and Cesnik [13]. The procedure followed here is similar to the one described in the cited work, with a few differences:

- Large rotations are taken into account for the evaluation of the local angle of attack during the on-line stage of the computation;
- Modal aerodynamic forces are calculated for the aeroelastic loop, instead of global aerodynamic coefficients.

3 Model Description

For this work, the following structure was considered: a high-aspect-ratio uniform wing of semi-span 16 m and chord 1 m, with a NACA 0012 profile, developed in Ritter *et al.* [8]. Its structural FE model is a beam with 32 elements of varying stiffness and lumped masses. The coordinates system is the one presented in Fig.1. The reference axis passes through 35% of the chord.

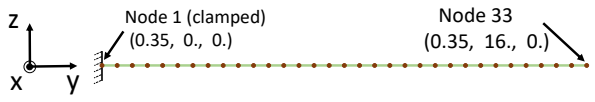

Fig. 1 Nastran structural beam model of the 16-m wing.

All reference structural solutions for the fitting of nonlinear displacements and forces in the ICE method were obtained using the Nastran SOL 400 solution.

The aerodynamic solutions used for the comparisons were obtained using the CFL3D code, a public-domain solver [15]. This originally included a linear modal solution which was modified to incorporate the ICE reduced order nonlinear modal method. The modifications are described in Medeiros *et al.* [14].

The aerodynamic mesh is structured, with a total of 2,490,210 cells. An illustration with the undeformed wing and the mesh is presented in Fig. 2.

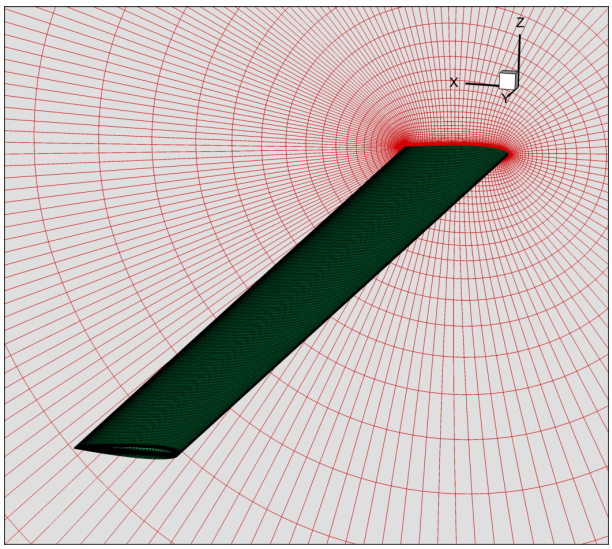

Fig. 2 CFL3D structured mesh for the 16-m wing.

Both steady and unsteady solutions were obtained using a Reynolds-averaged Navier-Stokes (RANS) approach, with a Spallart-Allmaras turbulence model [17]. The computation was parallel, with the domain sub-divided in 44 blocks.

4 Verification of the Structural ROM

This section briefly compares results obtained with the structural ROM and reference solutions obtained from Nastran SOL 400.

The structural ROM was identified from the original Nastran beam. The first 12 linear modes were considered, along with 10 additional dual

modes. For the training of this model, a total of 12,480 nonlinear static results were computed, using loads in the shape of each of the first 12 linear modes and pair combinations of them. The nonlinear forces and displacements are described by neural network functions.

Starting from the undeformed straight beam, a tip vertical force of 2 kN and an in-plane force of 1 kN were simultaneously applied at time $t = 0$. Figure 3 shows the tip response of the wing, comparing all three translation components with their counterparts obtained using Nonlinear nonlinear ("Nastran") and linear ("Linear") solutions.

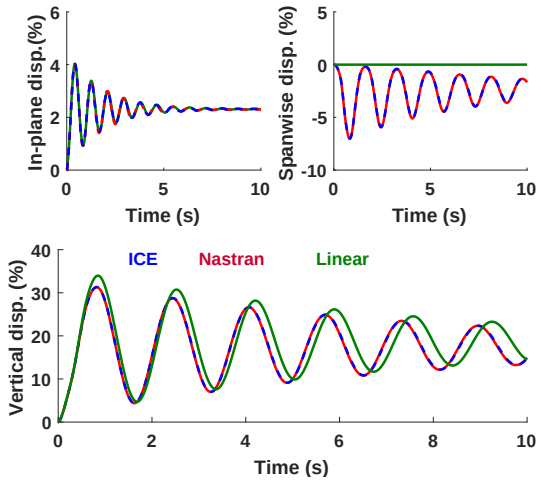

Fig. 3 Structural response after a step force is applied at the tip with 2 kN along the vertical direction (z axis) and 1 kN along the in-plane direction (x axis).

In this case, with maximum tip displacements in the order of 30% of the semi-span, the ROM solution showed excellent accuracy, following the nonlinear reference in all three translation components. It is important to see that the shortening of the projection in the spanwise direction with high displacements is a nonlinear feature of the motion, and that is why there is no linear response in that direction. For the vertical displacement, there are differences between the nonlinear and linear responses both in magnitude and phase, but the ROM really matched the nonlinear response in all aspects.

5 Aeroelastic Results

This section outlines the main results obtained with the combination MoS/ICE, a framework where the method of segments provides the aerodynamic loads for the structural solution obtained using the ROM. For the MoS, reference steady solutions were obtained with angles of attack up to 15 degrees, past the stall angle, and the step responses were obtained for small perturbations in the shape of the first 12 linear modes, the same ones considered for the structural ROM.

At this point, it is assumed that the structural model was properly verified against Nastran nonlinear solutions. Therefore, all comparisons have the objective to verify the aerodynamic solution considering the CFL3D/ICE as the high-fidelity reference solution.

5.1 Aeroelastic Static Results

The first aeroelastic comparisons are for static cases. The wing was subjected to a freestream flow with speed 40 m/s and two different root angles of attack, to excite a small deflection and a high deflection, with nonlinear effects.

Figure 4 compares the final deformation obtained using the MoS/ICE framework and the reference solution calculated with CFL3D/ICE. Looking at the vertical and span-wise displacements, there is a good agreement between the predictions. In absolute numbers, the errors are higher for the large deflection condition. This decreasing accuracy was expected because the reference deformation used for the calculation of the aerodynamic loads at each segment was the straight undeformed wing. This reference condition may be adjusted according to the range of application of the analysis.

Since the MoS transfers all the forces and moments to the structural solution, it is important to also check the accuracy of the in-plane displacement. Table 1 compares the tip translations and rotations for the two angles of attack simulated. The translations are expressed as % of semi-span, while rotations are in degrees.

The tip vertical displacement shows good

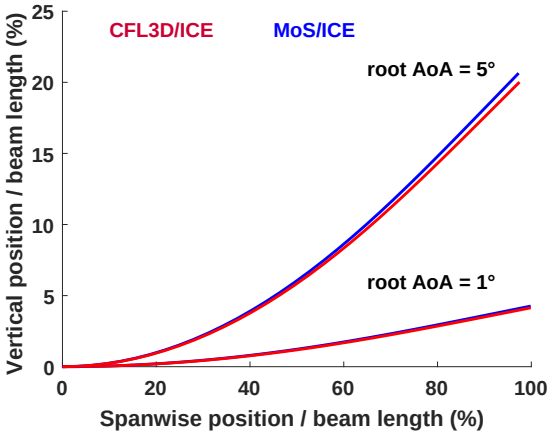

Fig. 4 Aeroelastic static comparisons for the 16-m wing at 40 m/s and two different root angles of attack.

comparison between the MoS/ICE and the CFL3D/MoS results with highest error lower than 0.6% of the wing semi-span. However, the in-plane displacements, in the x direction, and the in-plane rotation (around the z axis) have errors of 1.5% relative to the semi-span and 1.7 deg, respectively. In part, this error is due to the incomplete transfer of drag forces from using the method of segments. In fact, only the pressure drag is accounted for in the force balance. The friction drag is not yet included in the set of outputs used to generate the loads on the segments, since this would required additional post-processing.

Table 1 Comparison of tip displacements and rotations for the 16-m beam aeroelastic static solution at 40 m/s and different angles of attack.

AoA (deg)	1		5	
Method	CFD	MoS	CFD	MoS
In-plane disp. (%)	0.0	1.5	-0.4	0.8
Spanwise disp. (%)	-0.1	-0.1	-2.5	-2.7
Vertical disp. (%)	4.1	4.3	20.0	20.6
Rotation x (deg)	3.7	3.8	18.3	18.9
Torsion angle (deg)	0.0	0.2	0.2	0.7
Rotation z (deg)	0.0	-1.7	0.4	-1.1

5.2 Aeroelastic Dynamic Results

A first dynamic verification is a high-frequency tip moment excitation, starting from the 5-deg root AoA static condition. A sinusoidal moment of amplitude 10 kNm was applied about the y direction (torsion) with frequency close to the first torsion mode, 27.1 Hz, using a proportional damping of 2%. For this case, Fig. 5 shows a good match between the tip torsion angles obtained with the MoS/ICE framework and the CFL3D/ICE code.

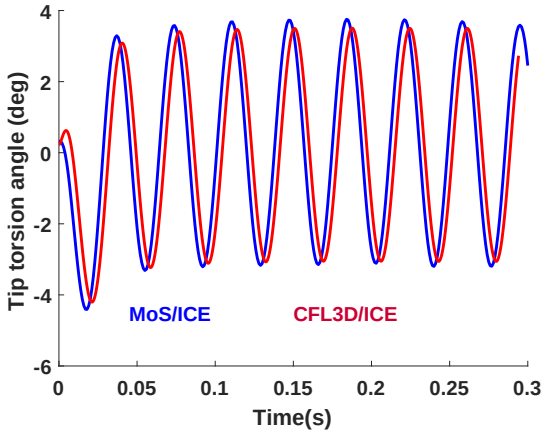

Fig. 5 Tip torsion angle comparison for a sinusoidal moment of ampitude 10 kNm.

The dynamic aeroelastic check for the MoS/ICE framework is to compare the unsteady large-displacement motion of the wing against a solution obtained with the CFL3D/ICE code. For this, a harmonic tip moment was applied about the y direction (torsion moment), inducing an angle of attack capable of generating lift for a large deflection simulation. The solution starts from the steady condition at 0-deg root AoA and the wingtip performs an oscillatory motion. This condition represents a typical low-frequency excitation for such high-aspect-ratio wings. The moment applied at the tip has amplitude of 6 kNm and the profile is a $1-cos$ function of frequency 0.5 Hz. The freestream velocity is 40 m/s, as in the steady cases, and the structure has a proportional damping of 2%. The tip displacements are presented in Fig. 6. In this case, the vertical

component achieves a maximum value around 24% of the semi-span at the first peak. The simulation time of the reference CFL3D/ICE solution is short, only 1.9 s, but the agreement between the high-fidelity aerodynamic solution and the plots obtained with the MoS was reasonable for this initial motion, considering all three displacement components. If only small disturbances relative to a given configuration are desired, it is possible to adopt a deformed reference condition. That would possibly increase the quality of the predictions for large displacements.

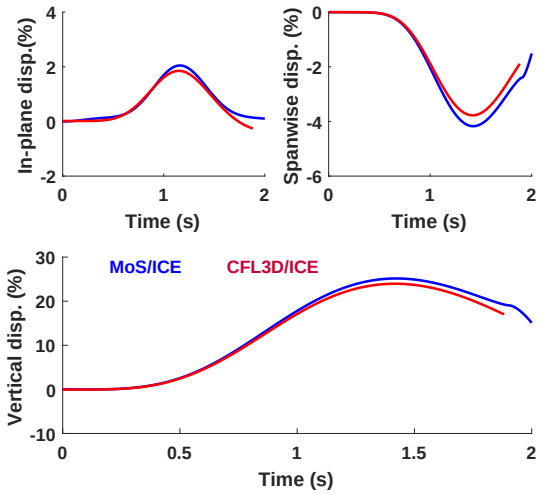

Fig. 6 Tip displacement following the application of an harmonic torsion moment of 6 kNm and 0.5 Hz.

Comparing the tip twist angle, there is a good agreement between the MoS/ICE prediction and the solution obtained with the CFL3D/ICE framework, as shown in Fig. 7. The twist angle goes up to approximately 14 degrees, indicating that nonlinear phenomena are already playing a role in the aeroelastic solution. In fact, the tip twist angle obtained from the MoS with pure convolution without any correction factor is at a lower level and has higher frequency when compared to its nonlinear counterparts. This result also shows that using a linear solution for aeroelastic analysis involving large displacements may not be a conservative approach in terms of loads and angle of attack predictions.

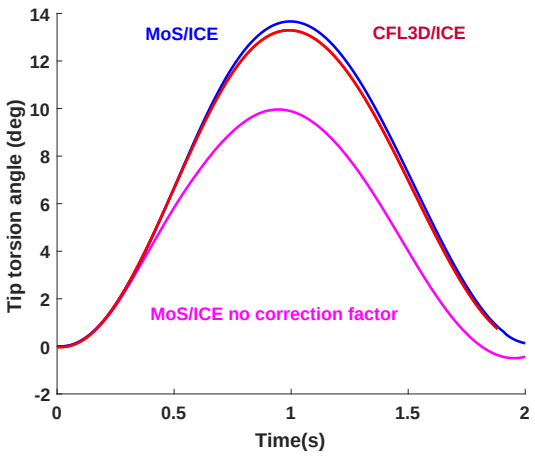

Fig. 7 Tip twist angle following the application of an harmonic torsion moment of 6 kNm and 0.5 Hz.

The major benefit from the MoS is the decreased computational cost compared to the CFD solution. Running the high-fidelity solution with an adequate time step for only 1.9 s using 45 cores takes 27 hours, while the same solution using the MoS/ICE framework in Matlab takes 7 minutes. For a reduced order model, 7 min. is a relatively long time, but there is potential to decrease this time significantly by selecting suitable samples for the time step responses used in the convolution. In fact, the convolution is the most time-consuming task in the MoS calculation.

6 Conclusions

This work presented the integration of an aeroelastic framework that uses reduced order models capable of dealing with large displacements for both the structural and the aerodynamic solutions. The structural approach is based on the Implicit Condensation and Expansion method, with the addition of large nonlinear displacement for the inertia forces calculation, while the aerodynamic solution is based on the method of segments, including a combination of linear convolution with a correction factor to account for nonlinear effects.

The accuracy of the structural solutions was verified through comparisons between Nastran

SOL 400 nonlinear results and ICE predictions. Static and dynamic aeroelastic solutions indicated a good agreement between the CFL3D predictions and the results obtained with the MoS. As expected, most of the overall error of the aeroelastic solution is due to the aerodynamic reduced order model. However, employing a correction factor on top of a linear convolution from step responses proved to be a good strategy for dealing with large displacements and angles of attack, correcting the linear response in phase and amplitude.

At the end, significant reductions in simulation time were achieved by using the reduced order models when compared to the high-fidelity one. Accuracy can be increased in future investigations by adjusting the reference condition around which the correction factors are evaluated.

References

[1] Shearer C M and Cesnik C E S. Nonlinear Flight Dynamics of Very Flexible Aircraft. *Journal of Aircraft*, Vol. 44, No. 5, pp. 1528–1545, 2007.

[2] Drela M. Integrated simulation model for preliminary aerodynamic, structural, and control-law design of aircraft. In *40th Structures, Structural Dynamics, and Materials Conference and Exhibit*, Structures, Structural Dynamics, and Materials and Co-located Conferences. American Institute of Aeronautics and Astronautics, 1999. doi:10.2514/6.1999-1394.

[3] McEwan M I, Wright J R, Cooper J E and Leung A Y T. A combined modal/finite element analysis technique for the dynamic response of a non-linear beam to harmonic excitation. *Journal of Sound and Vibration*, Vol. 243, No. 4, pp. 601–624, 2001.

[4] Mignolet M P and Soize C. Stochastic Reduced Order Models for Uncertain Geometrically Nonlinear Dynamical Systems. *Computer Methods in Applied Mechanics and Engineering*, Vol. 197, No. 45, pp. 3951–3963, 2008. doi: 10.1016/j.cma.2008.03.032.

[5] Hollkamp J J and Gordon R W. Reduced-order models for nonlinear response prediction: Implicit condensation and expansion. *Journal of Sound and Vibration*, Vol. 318, No. 4, pp. 1139–1153, 2008.

[6] Noll T E, Brown J M, Perez-Davis M E, Ishmael S D, Tiffany G C and Gaier M. Investigation of the Helios Prototype Aircraft Mishap. Technical Report Volume I - Mishap Report, NASA, January 2004.

[7] Jones J R and Cesnik C E S. Preliminary flight test correlations of the X-HALE aeroelastic experiment. *The Aeronautical Journal*, Vol. 119, No. 1217, pp. 855–870, 2015. doi: 10.1017/S0001924000010952.

[8] Ritter M, Cesnik C E S and Krüger W R. An enhanced modal approach for large deformation modeling of wing-like structures. In *AIAA Science and Technology Forum and Exposition (SciTech2015), 56th AIAA/ASCE/AHS/ASC Structures, Structural Dynamics, and Materials Conference*. 2015. Kissimmee, Florida, 5-9 January 2015. AIAA 2015-0176, 10.2514/6.2015-0176.

[9] Medeiros R M, Cesnik C E S and Coetzee E B. Modal formulation for geometrically nonlinear structural dynamics. In *International Forum on Aeroelasticity and Structural Dynamics (IFASD 2017)*. 2017. Como, Italy, 25-28 June 2017.

[10] Taira K, Brunton S L, Dawson S T M, Rowley C W, Colonius T, McKeon B J, Schmidt O T, Gordeyev S, Theofilis V and Ukeiley L S. Modal analysis of fluid flows: An overview. *AIAA Journal*, pp. 1–29, 2017.

[11] Mannarino A and Dowell E. Reduced-order models for computational-fluid-dynamics-based nonlinear aeroelastic problems. *AIAA Journal*, Vol. 53, pp. 2671–2685, 2015. doi:10.2514/1.J053775.

[12] Winter M and Breitsamter C. Efficient unsteady aerodynamic loads prediction based on nonlinear system identification and proper orthogonal decomposition. *Journal of Fluids and Structures*, Vol. 67, No. Supplement C, pp. 1–21, 2016.

[13] Skujins T and Cesnik C E S. Reduced-Order Modeling of Unsteady Aerodynamics Across Multiple Mach Regimes. *Journal of Aircraft*, Vol. 51, No. 6, pp. 1681–1704, 2014.

[14] Medeiros R R, Cesnik C E S and Coetzee E B. Nonlinear Computational Aeroelastic-

ity Using Structural Modal Coordinates. In *2018 AIAA/ASCE/AHS/ASC Structures, Structural Dynamics, and Materials Conference*, AIAA SciTech Forum. American Institute of Aeronautics and Astronautics, 2018.

[15] Bartels R E, Rumsey C L and Biedron R T. Cfl3d version 6.4-general usage and aeroelastic analysis. Technical Report NASA/TM-2006-214301, NASA Langley Research Center, 2006.

[16] Medeiros R M, Cesnik C E S and Coetzee E B. Modal formulation for geometrically nonlinear structural dynamics. In *International Forum on Aeroelasticity and Structural Dynamics (IFASD)*. Como, Italy, 25-28 June 2017.

[17] Spalart P and Allmaras S. A one-equation turbulence model for aerodynamic flows. In *30th Aerospace Sciences Meeting and Exhibit*, Aerospace Sciences Meetings. American Institute of Aeronautics and Astronautics, 1992.

7 Contact Author Email Address

Contact author: Renato R. Medeiros
Mail to: renatorm@umich.edu

Acknowledgements

This work is supported by Airbus Americas Inc., with David Hills as the Airbus Project Leader. Technical discussions with him are greatly appreciated. The first author also acknowledges the support of CNPq (Conselho Nacional de Desenvolvimento Científico e Tecnológico, Brazil) and the University of Michigan for his academic scholarship.

Copyright Statement